An Active Acoustic Metamaterial With Tunable Effective Density

Amr M. Baz
Department of Mechanical Engineering,
University of Maryland,
2137 Engineering Building,
College Park, MD 20742
e-mail: baz@umd.edu

Extensive efforts are being exerted to develop various types of acoustic metamaterials to effectively control the flow of acoustical energy through these materials. However, all these efforts are focused on passive metamaterials with fixed material properties. In this paper, the emphasis is placed on the development of a class of one-dimensional acoustic metamaterials with tunable effective densities in an attempt to enable the adaptation to varying external environment. More importantly, the active metamaterials can be tailored to have increasing or decreasing variation of the material properties along and across the material volume. With such unique capabilities, physically realizable acoustic cloaks can be achieved and objects treated with these active metamaterials can become acoustically invisible. The theoretical analysis of this class of active acoustic metamaterials is presented and the theoretical predictions are determined for an array of fluid cavities separated by piezoelectric boundaries. These boundaries control the stiffness of the individual cavity and in turn its dynamical density. Various control strategies are considered to achieve different spectral and spatial control of the density of this class of acoustic metamaterials. A natural extension of this work is to include active control capabilities to tailor the bulk modulus distribution of the metamaterial in order to build practical configurations of acoustic cloaks. [DOI: 10.1115/1.4000983]

Keywords: active acoustic metamaterials, programmable metamaterials, acoustic cloaks

1 Introduction

The development of metamaterials with optical, electromagnetic, and acoustical properties that are unachievable with natural materials have attracted considerable interest during the last decade [1–3]. In particular, the development of the acoustic metamaterials has been motivated by the need for understanding the underlying phenomena governing the operation and practical realization of effective acoustic cloaks that can be used for treating critical objects in order to render them acoustically invisible. An excellent review of the basic phenomena and the history of development of cloaking are presented by Milton et al. [4].

The pioneering work of Cummer and Schurig [5] established theoretically that two-dimensional acoustic cloaks are possible through the use of acoustic materials that have strong anisotropy, which do not exist in nature. Since then extensive efforts have been exerted to broaden the theoretical foundation and investigate possible means for realization of effective acoustic cloaks. Distinct among these efforts are the works of Cummer et al. [6] and Norris [7] about the basics of the theory of acoustic cloaking. Torrent and Sanchez-Dehesa [8,9] comprehensively investigated the theory governing the development of multilayered in order to achieve the anisotropy requirements presented by Cummer and Schurig [5]. Other efforts along the same direction have been carried out by Popa and Cummer [10], Cheng and co-workers [11,12], and Cheng and Liu [13] to study either two- and/or three-dimensional layered metamaterials. The improved design of the acoustic cloaking using an impedance matching approach is proposed by Chen et al. [14] in order to avoid the infinite mass problem of the ideal cloak of Cummer et al. [15].

Acoustic metafluids consisting of layered composite media have also been considered. These metafluids have either anisotropic density and scalar bulk modulus [16] or anisotropic density and bulk modulus [17].

Unlike the extensive theoretical studies of acoustic metamaterials, the experimental investigations are by far lacking. However, an important experimental study that is relevant to this paper is the work of Lee and co-workers [18,19], which demonstrated the negative effective density characteristics of an acoustic metamaterial consisting of an array of cavities separated by thin elastic membranes. Similar results were reported by Yao et al. [20] using a spring-mass system.

In all the above studies, the focus has been placed on passive metamaterials with fixed material properties. This limits considerably the potential of these materials. In this paper, the emphasis is placed on the development of a class of one-dimensional acoustic metamaterials with tunable effective densities, which can be tailored to have increasing or decreasing variation along the material volume. With such unique capabilities, physically realizable acoustic cloaks can be achieved and objects treated with these active metamaterials can become acoustically invisible.

This paper is organized in seven sections. In Sec. 1, a brief introduction is presented. In Sec. 2, the concept of the active acoustic metamaterial is introduced. In Secs. 3–5, lumped-parameter models of plain cavities, cavities with flexible diaphragms, and cavities with piezoelectric diaphragms are outlined in order to motivate the need for the active component to achieve a "programmable" acoustic metamaterial. In Sec. 6, numerical examples are considered to demonstrate the performance characteristics of the active metamaterial. A brief summary of the conclusions and the future work are outlined in Sec. 7.

2 Concept of Active Acoustic Metamaterial

2.1 Why Active Acoustic Metamaterial?. In order to understand the need for an active acoustic metamaterial, consider the passive acoustic cloak shown in Fig. 1.

For an ideal cloak, the required distribution of the density (ρ_r and ρ_θ in the radial and tangential directions) and bulk modulus (κ) are given by [5]

Contributed by the Technical Committee on Vibration and Sound of ASME for publication in the Journal of Vibration and Acoustics. Manuscript received July 21, 2009; final manuscript received December 10, 2009; published online xxxxx-xxxxx-xxxxx. Assoc. Editor: Noel C. Perkins.

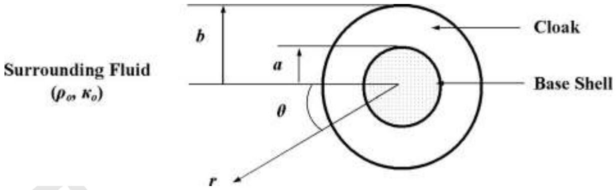

Fig. 1 Acoustic cloak

$$\frac{\rho_r}{\rho_o} = \frac{r}{r-a}, \quad \frac{\rho_\theta}{\rho_o} = \frac{r-a}{r}, \quad \text{and} \quad \frac{\kappa_o}{\kappa} = \left(\frac{b}{b-a}\right)^2 \frac{r-a}{r} \tag{1}$$

As there are no natural materials that have these idealized distributions of physical properties, multilayered composite cloaks have been proposed as a possible means for physically realizing such distributions [8,9,11,12]. Figure 2 shows a possible configuration of such a composite, which is made of two isotropic materials A and B.

When $d_b/d_a=1$ and $b/a=2$, the idealized properties are related to the physical properties of the stacked materials A and B by the following rules of mixtures [11,12]:

$$\rho_r' = \frac{1}{2}(\rho_A' + \rho_B'), \quad \rho_\theta' = 2\frac{\rho_A'\rho_B'}{(\rho_A' + \rho_B')}, \quad \text{and} \quad \kappa' = 2\frac{\kappa_A'\kappa_B'}{(\kappa_A' + \kappa_B')} \tag{2}$$

where $\rho_i'=\rho_i/\rho_o$ and $\kappa_i'=\kappa_i/\kappa_o$. Hence, for any values of the idealized densities ρ_r' and ρ_θ', the first two identities of Eq. (2) are solved simultaneously to extract the physically realizable densities ρ_A' and ρ_B' as follows:

$$\rho_A' = \rho_r' - \sqrt{\rho_r'^2 - 1} \quad \text{and} \quad \rho_B' = \rho_r' + \sqrt{\rho_r'^2 - 1} \tag{3}$$

Note that in deriving Eq. (3), Eq. (1) is used as it implies that $\rho_r'=1/\rho_\theta'$.

Equations (1)–(3) are used to plot the distributions of ρ_A', ρ_B', and κ' along the radius r of the cloak as shown in Fig. 3. The figure indicates that the realization of an acoustic cloak, which consists of multilayer passive isotropic materials require the use of materials that have densities and bulk modulus varying many orders of magnitude along the cloak. Furthermore, one of the constituents of the cloak has its density increasing along the cloak whereas the second constituent has its density decreasing. Practical realization of such a cloak configuration is very difficult with current materials if not impossible.

Therefore, a radically different approach is essential to realizing the desired acoustic cloak. In this paper, an active acoustic metamaterial is proposed to overcome such challenging limitations of passive cloaks.

2.2 A Configuration of the Active Acoustic Metamaterial. Figure 4 displays a configuration of the acoustic cloak, which consists of an array of fluid cavities separated by piezoelectric boundaries. The displayed configuration is a rectangular approximation of a slice taken at section 1-1 of Fig. 2. The exact tapered configuration is being analyzed in a separate study by the author. Mechanically, each unit cell of this array is identical to the other unit cell, which makes the physical realization of this concept rather feasible. However, electrically, the piezoelectric boundaries are controlled separately in order to achieve increasing or decreasing dynamical density distributions that can also vary by many orders of magnitudes along the array. Various control strategies can be considered to achieve different spectral and spatial control of the density of this class of acoustic metamaterials.

Note that the proposed configuration of the active metamaterial is limited only to generating controlled effective densities. In future studies, other configurations will be developed to generate controlled effective bulk modulus.

Analysis of the proposed active acoustic metamaterial is preceded by the analysis of plain cavities and then cavities with passive diaphragms in order to emphasize their limitations and motivate the need for the active component to achieve a programmable acoustic metamaterial.

3 Plain Acoustic Cavity

Consider the plain acoustic cavity shown in Fig. 5. The dynamical equation of the plain cavity is obtained by applying Kirchhoff's voltage law on its equivalent electrical analog to give

$$\frac{\rho_o l}{A}\frac{dQ}{dt} + \frac{\rho_o c_o^2}{V}\int Q dt = -\Delta p \tag{4}$$

In the Laplace domain, Eq. (4) becomes

$$\left(\frac{\rho_o l}{A}s + \frac{\rho_o c_o^2}{V}\frac{1}{s}\right)Q = -\Delta P \tag{5}$$

Equation (5) can be rewritten as

$$\Delta P/l = -\rho_o\left(1 + \frac{c_o^2}{l^2}\frac{1}{s^2}\right)su \tag{6}$$

where $u=Q/A$ is the fluid velocity. Equation (6) is in a form of Euler's equation [21,22] indicating that the fluid has an effective density ρ_{eff} given by

$$\rho_{\text{eff}}/\rho_o = \left(1 + \frac{c_o^2}{l^2}\frac{1}{s^2}\right) \tag{7}$$

For sinusoidal excitation at a frequency ω, Eq. (7) reduces to

$$\rho_{\text{eff}}/\rho_o = \left(1 - \frac{c_o^2}{l^2}\frac{1}{\omega^2}\right) \tag{8}$$

4 Acoustic Cavity With Flexible Diaphragm

Now, let us consider the acoustic cavity with flexible diaphragm shown in Fig. 6. This arrangement is similar to the experimental set-up conceived by Lee et al. [18].

The dynamical equation of an acoustic cavity with flexible diaphragm is obtained using Kirchhoff's voltage law. This equation is given in the Laplace domain by

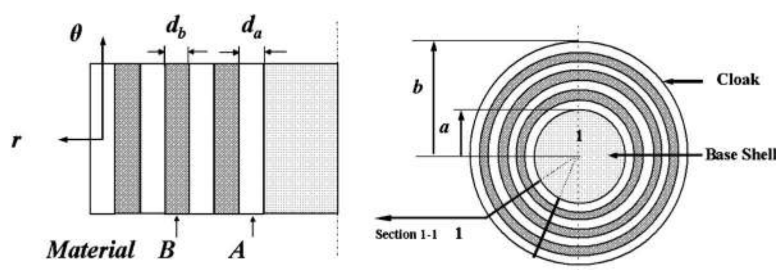

Fig. 2 Multilayered acoustic cloak

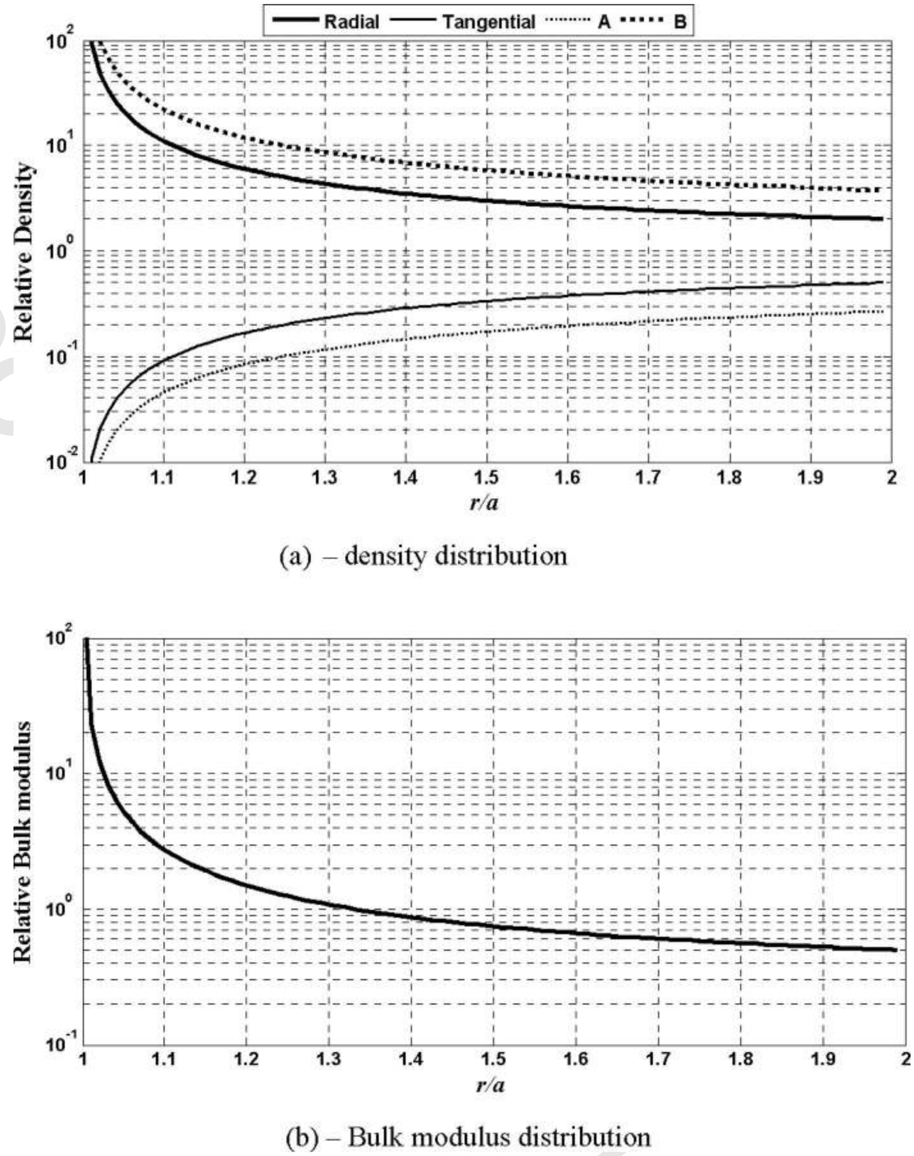

Fig. 3 Density and bulk modulus distributions

$$\left(\frac{\rho_o l}{A}s + \frac{1}{C_D}\frac{1}{s}\right)Q = -\Delta P \qquad (9)$$

Equation (9) can be rewritten as

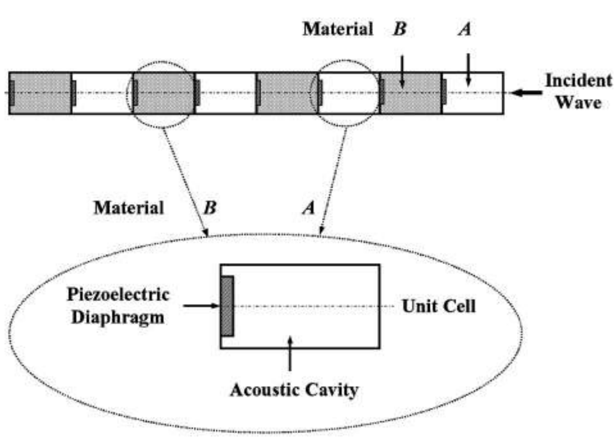

Fig. 4 Configuration of active acoustic metamaterial

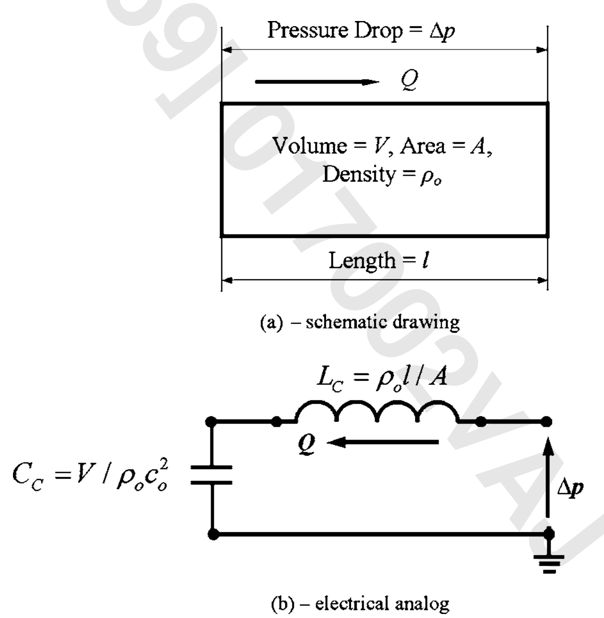

Fig. 5 Plain acoustic cavity

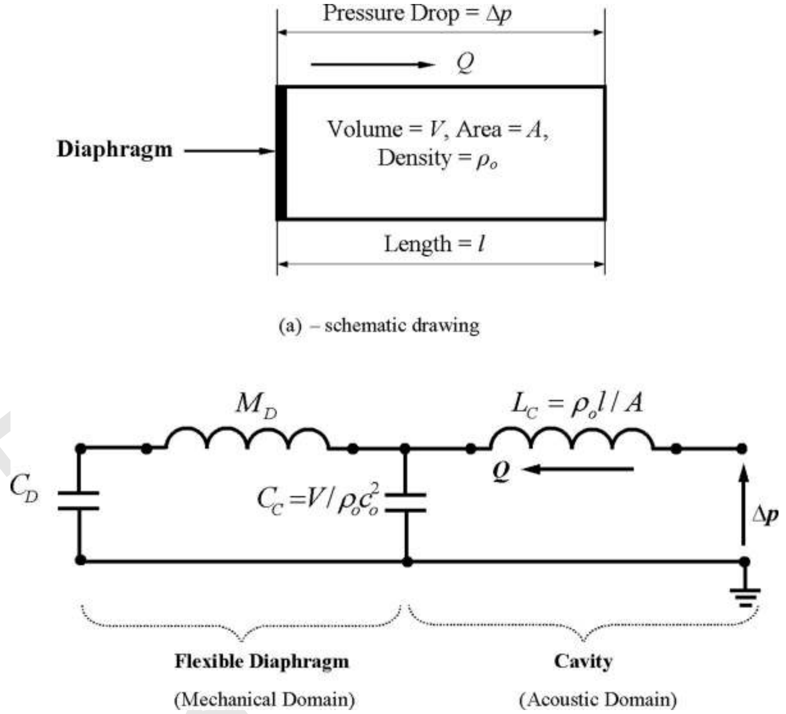

Fig. 6 Acoustic cavity with flexible diaphragm

$$\Delta P/l = -\rho_o\left(1 + \frac{A}{l\rho_o C_D}\frac{1}{s^2}\right)su \tag{10}$$

Hence, the effective dynamical density of a fluid inside a cavity with a flexible diaphragm is given by

$$\rho_{\text{eff}}/\rho_o = 1 + \frac{A}{l\rho_o C_D}\frac{1}{s^2} = 1 + \frac{k_D}{\rho_o s^2} \tag{11}$$

where $k_D = A/lC_D$ is the diaphragm stiffness.

Equation (11) suggests that ρ_{eff} depends on both the diaphragm stiffness k_D and the frequency ω. Therefore, ρ_{eff} can be set to a particular value by selecting k_D while operating at a fixed frequency ω_o. However, operating at frequencies other than ω_o will result in dramatic changes in the value of ρ_{eff}.

5 Acoustic Cavity With Piezoelectric Diaphragm

5.1 Basic Equations. Consider the acoustic cavity with piezoelectric diaphragm shown in Fig. 7. The basic constitutive equation for a piezoelectric material [23] is given by

$$\begin{Bmatrix} S \\ D \end{Bmatrix} = \begin{bmatrix} s^E & d \\ d & \varepsilon \end{bmatrix}\begin{Bmatrix} T \\ E \end{Bmatrix} \tag{12}$$

where S is the strain, D is the electrical displacement, T is the stress, E is the electrical field, s^E is the compliance, d is the piezoelectric strain coefficient, and ε is the permittivity. Equation (12) can be rewritten [24] as

$$\begin{Bmatrix} \Delta\text{Vol} \\ q \end{Bmatrix} = \begin{bmatrix} C_D & d_A \\ d_A & 1/Z_P s \end{bmatrix}\begin{Bmatrix} \Delta p_P \\ V_P \end{Bmatrix} \tag{13}$$

where ΔVol is the change in diaphragm volume, q is the electrical charge, Δp_P is the pressure across piezoelectric diaphragm, and V_P is the voltage. Also, C_D is the diaphragm compliance and Z_P is the impedance of piezoelectric diaphragm and attached elements given by

$$Z_P = [(L_P s)/\{1 + L_P C_P C_s s^2/(C_P + C_s)\}] \tag{14}$$

where C_P is the capacitance of piezoelectric diaphragm, which is $A\varepsilon/t$ with A as the diaphragm area and t is the diaphragm thickness. Also, L_P denotes a shunted inductance *in-parallel* with the piezoelectric diaphragm and C_s denotes a capacitance *in-series* with the piezoelectric diaphragm.

Using the piezoelectric diaphragm as a self-sensing actuator, then the second row of Eq. (13) gives, for a short-circuit piezoelectric sensor, the following expression:

$$q = d_A \Delta p_P \tag{15}$$

Then, the voltage V_P applied to the piezoelectric diaphragm can be generated by a direct feedback of the charge q such that

$$V_P = -G d_A \Delta p_P \tag{16}$$

where G is the feedback gain.

Then, the first row of Eq. (13) yields

$$\Delta\text{Vol} = (C_D - d_A^2 G)\Delta p_P = C_{DC}\Delta p_P \tag{17}$$

where C_{DC} is the closed-loop compliance of piezoelectric diaphragm.

Figure 8 displays the corresponding electrical analog of the acoustic cavity with closed-loop piezoelectric diaphragm.

The transfer function of the controlled cavity system, relating the flow velocity u to the pressure drop ΔP is given by

$$\frac{\Delta p}{l} = -\rho_0\left[1 + \frac{C_{DC}T + 1}{L_C s^2(C_{DC} + C_C[C_{DC}T + 1])}\right]su \tag{18}$$

where

$$T = M_D s^2 + Z_P' s \tag{19}$$

with

$$Z_P' = Z_P \phi^2 \tag{20}$$

Equation (18) yields the following expression for the effective density ρ_{eff}:

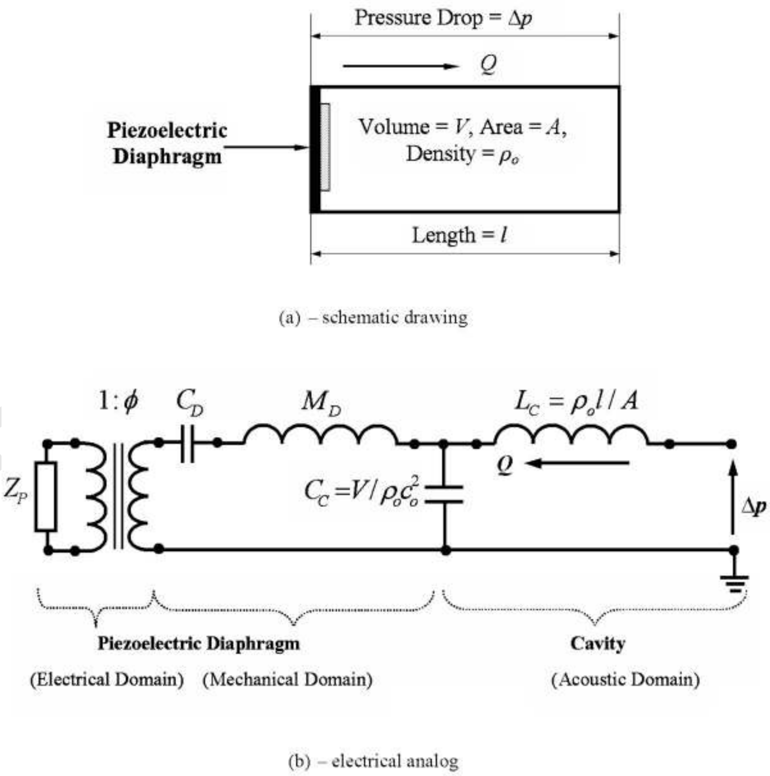

Fig. 7 Acoustic cavity with open-loop piezoelectric diaphragm

$$\rho_{\text{eff}} = \rho_0\left[1 + \frac{C_{DC}T + 1}{L_C s^2(C_{DC} + C_C[C_{DC}T + 1])}\right] \quad (21)$$

5.2 Analysis of the Effective Density. The two following limiting cases are considered:

I. If $M_D \approx 0$ (i.e., mass of diaphragm is negligible), then Eq. (21) reduces to

$$\rho_{\text{eff}}/\rho_o \cong \left[1 + \frac{C_{DC}Z'_P s + 1}{L_C s^2[C_{DC} + C_C(C_{DC}Z'_P s + 1)]}\right] \quad (22)$$

From Eq. (22), two subcases can be identified as follows:

Case A: $C_{DC} \to 0$, i.e., a rigid diaphragm case, Eq. (21) becomes

$$\rho_{\text{eff}}/\rho_o \cong \left[1 + \frac{1}{L_C C_C s^2}\right] = \left[1 + \frac{c_o^2}{l^2 s^2}\right] \quad (23)$$

which is the same as Eq. (7).

Case B: $C_C \to 0$, i.e., incompressible case

a. No piezoelectric effect, Eq. (22) becomes

$$\rho_{\text{eff}}/\rho_o \cong \left[1 + \frac{1}{L_C C_D s^2}\right] = \left[1 + \frac{k_D}{\rho s^2}\right] \quad (24)$$

which is the same as Eq. (11).

b. With piezoelectric effect, Eq. (21) yields

$$\rho_{\text{eff}}/\rho_o \cong \left[1 + \frac{C_{DC}Z'_P s + 1}{L_C C_{DC} s^2}\right] \quad (25)$$

If $\rho_{\text{eff}}/\rho_o = \rho'_d$ then Eq. (25) yields the following expression for the feedback gain G

$$G = \frac{(\rho'_d - 1)L_C C_D s^2 - C_D Z'_P s - 1}{d_A^2[(\rho'_d - 1)L_C s^2 - Z'_P s]} \quad (26)$$

This gain ensures that $\rho_{\text{eff}}/\rho_o = \rho'_d$ for any frequency ω.

From Eq. (26), three distinct points can be distinguished.

i. At $s=0$ (i.e., $\omega=0$), $G=\infty$. Hence, very large control voltage is needed to maintain a desired density at low frequencies.
ii. At $s=\infty$ (i.e., $\omega=\infty$), $G=C_D/d_A^2$. This suggests that the control voltage assumes a constant value at high frequencies.
iii. $G=0$ at a value s_o, which satisfies

$$(\rho'_d - 1)L_C C_D s_o^2 - C_D Z'_{P_o} s_o - 1 = 0 \quad (27)$$

At such a specific frequency s_o, the desired density ρ'_d can be attained completely passively without the need for any active control (i.e., $G=0$). Note that Z'_{P_o} is the value of the impedance at s_o, i.e., $Z'_{P_o} = [(L_P s_o)/\{1 + L_P C_P C_s s_o^2/(C_P + C_s)\}]\phi^2$.

II. If $M_D \gg 0$ (i.e., mass of diaphragm is not negligible), then Eq. (21) reduces to

$$G = \frac{(\rho'_d - 1)L_C s^2(C_C + C_D + C_C C_D T) - C_D T - 1}{d_A^2[(\rho'_d - 1)L_C s^2(1 + C_C T) - T]} \quad (28)$$

Equation (28) gives the gain for the general case of a cavity with flexible piezoelectric diaphragm. The gain has a fourth-order characteristics equation. It reduces to a third-order equation when $M_D \approx 0$ as given by Eq. (26). The prediction accuracy of the

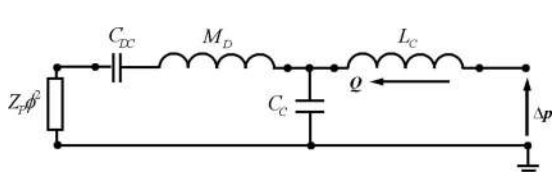

Fig. 8 Acoustic cavity with closed-loop piezoelectric diaphragm

Table 1 Parameters of acoustic cavity/piezoelectric diaphragm system

Parameter	Value
ϕ	138.3 Pa/V
C_D	1.5243×10^{-13} $m^4\ s^2/kg$
M_D	13,456 kg/m^4
d_A	-2.1080×10^{-11} m^3/V
C_P	18.239 nF
C_C	1.8466×10^{-15} $m^4\ s^2/kg$
L_C	24,069 kg/m^4

reduced-order feedback gain equation will be presented in Sec. 6.

6 Numerical Performance of an Acoustic Cavity With Piezoelectric Diaphragm

Consider an acoustic cavity ($l=0.01$ m, $A=4.15\times10^{-4}$ m^2), filled with water ($\rho_o=1000$ kg/m^3, $c_o=1500$ m/s) and coupled with a piezoelectric diaphragm that has the characteristics listed in Table 1 [24].

Figure 9 shows a comparison between the dimensionless density $\rho_{\rm eff}/\rho_o$ for a passive cavity with flexible diaphragm ($G=0$) and a cavity with piezoelectric diaphragm, which is controlled to maintain $\rho_d'=20$. It can be seen that the passive cavity has a negative effective density, which is also continuously varying with the frequency as indicated in Fig. 9(*a*). This result conforms to the results reported by Lee et al. [18]. Ultimately, when the frequency $\omega\to\infty$, $\rho_d'=1$. Hence, the passive system cannot be tuned to $\rho_d'=20$. However, with the active cavity, the effective density is maintained at $\rho_d'=20$ when the appropriate control voltage is provided as shown in the middle graph of Fig. 9(*b*). Note that for a sound pressure level of 120 dB, the pressure $p=1$ Pa and the control voltage at a frequency of 10 Hz is 230 V. This control voltage drops considerably as the frequency is increased. The specific profile of the control voltage can be easily understood by considering the discussions following Eqs. (26) and (27). At a frequency of 570 Hz, the control voltage drops to zero indicating that the desired density ρ_d' can be attained completely passively without the need for any active control (i.e., $G=0$).

Note also that the closed-loop compliance C_{DC} is positive as shown in the bottom graph of Fig. 9(*b*). This is achieved only with active acoustic metamaterial case when $L_P=50H$ and $C_S=0.2pf$.

Consider now an active acoustic metamaterial consisting of, for example, the eight cells as shown in Fig. 4. Four of these cells are programmed to generate material ***A*** with increasing density distribution while the remaining four replicate material ***B*** with decreasing density distribution along the cloak.

Figure 10 shows the density and control voltage of the four discrete unit cells of material ***A*** in an attempt to approximate the idealized continuous ρ_A/ρ_o distribution. Figure 11 displays the corresponding characteristics of the four discrete unit cells of material ***B***, which approximate the idealized continuous ρ_B/ρ_o distribution.

More number of cells is obviously needed to accurately replicate the characteristics of the *A* and *B* materials.

Comparisons between the predictions of the full (exact) and reduced-order (approximate) feedback gain models are shown in Fig. 12 for values of $\rho_{\rm eff}/\rho_o$ of 30 and 0.075. It is evident that the predictions of the reduced-order model are in excellent agreement with those of the full-order model. This simplifies considerably the implementation of the active acoustic metamaterial.

7 Conclusions

This paper has presented a class of one-dimensional acoustic metamaterials with programmable densities. The active metamaterials are shown theoretically to be tunable to have increasing or decreasing density distributions along the material.

The theoretical analysis of this class of active acoustic metamaterials is presented for an array of air cavities separated by piezoelectric boundaries using a lumped-parameter modeling approach. Various control strategies are considered to achieve different spectral and spatial control of the density of this class of acoustic metamaterials. The comparisons are presented between the characteristics of the active and passive metamaterials to emphasize the potential of the active metamaterials for physically generating a wide range of effective densities in a simple and uniform manner.

It is important to note here that all the presented results are based on a single cell model. The effect of coupling between neighboring cells will be considered in future studies.

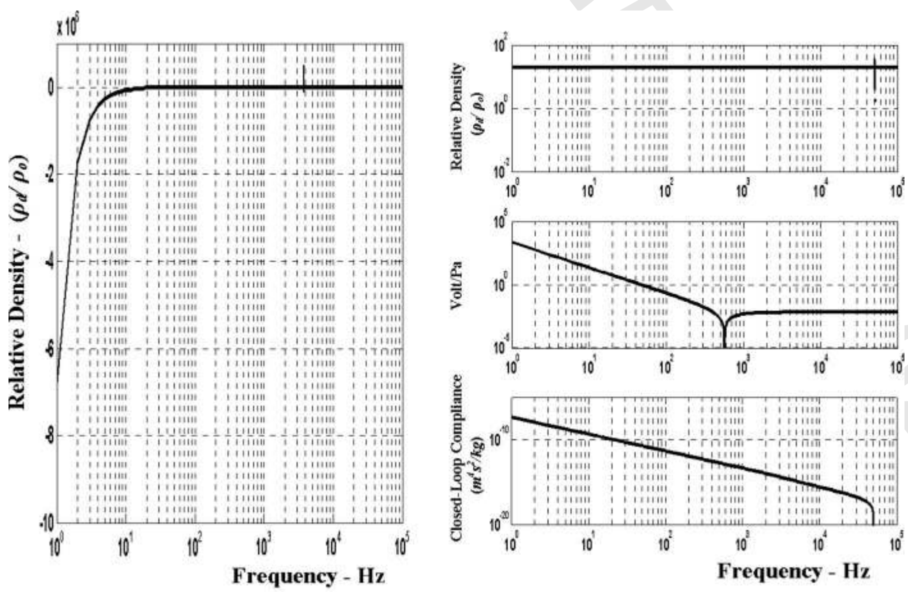

(a) – passive (G=0) (b) – active with $\rho_{eff}/\rho_o=20$

Fig. 9 Comparison between passive and active cavities

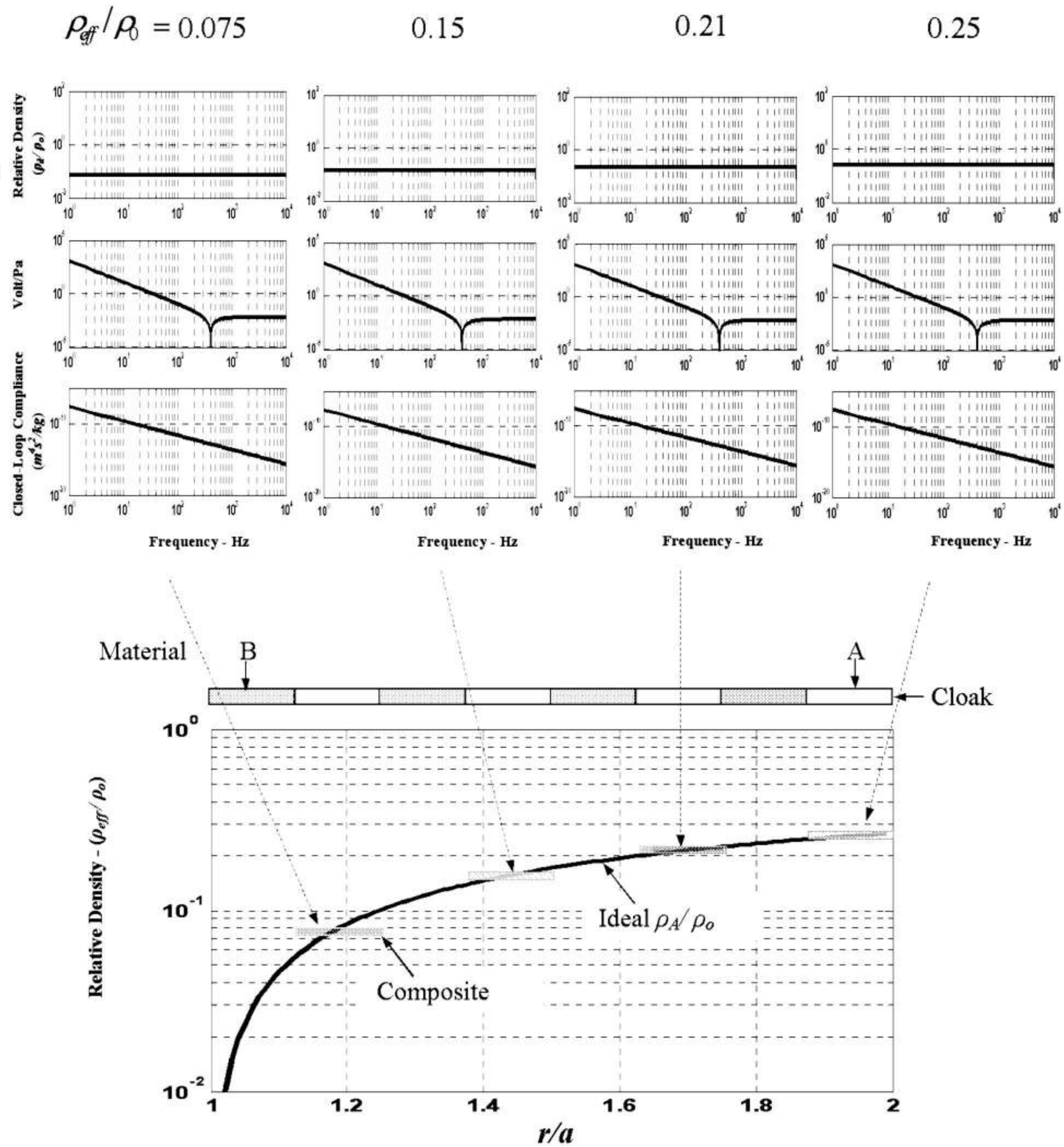

Fig. 10 Active acoustic metamaterial (*A*) with increasing density distribution

Also, a natural extension of this work is to include active control capabilities to tailor the bulk modulus distribution of the metamaterial.

Combining the tunable density and bulk modulus capabilities, will enable the physically realization of practical acoustic cloaks and objects treated with these active metamaterials can become acoustically invisible.

Acknowledgment

This work has been funded by a grant from the Office of Naval Research (Grant No. N000140910038). Special thanks are due to Dr. Kam Ng and Dr. Scott Hassan, the technical monitors, for their invaluable inputs and comments.

Nomenclature

A = area of cavity
C_C = compliance of cavity
C_D = open-loop compliance of diaphragm
C_{DC} = closed-loop compliance of diaphragm
C_P = capacitance of piezoelectric diaphragm
C_s = capacitance in-series with piezoelectric diaphragm
C_T = closed-loop compliance of diaphragm
c_o = sound speed
D = electrical displacement
d = piezoelectric strain coefficient
d_A = effective Piezoelectric Coefficient ($d_A = dA$)

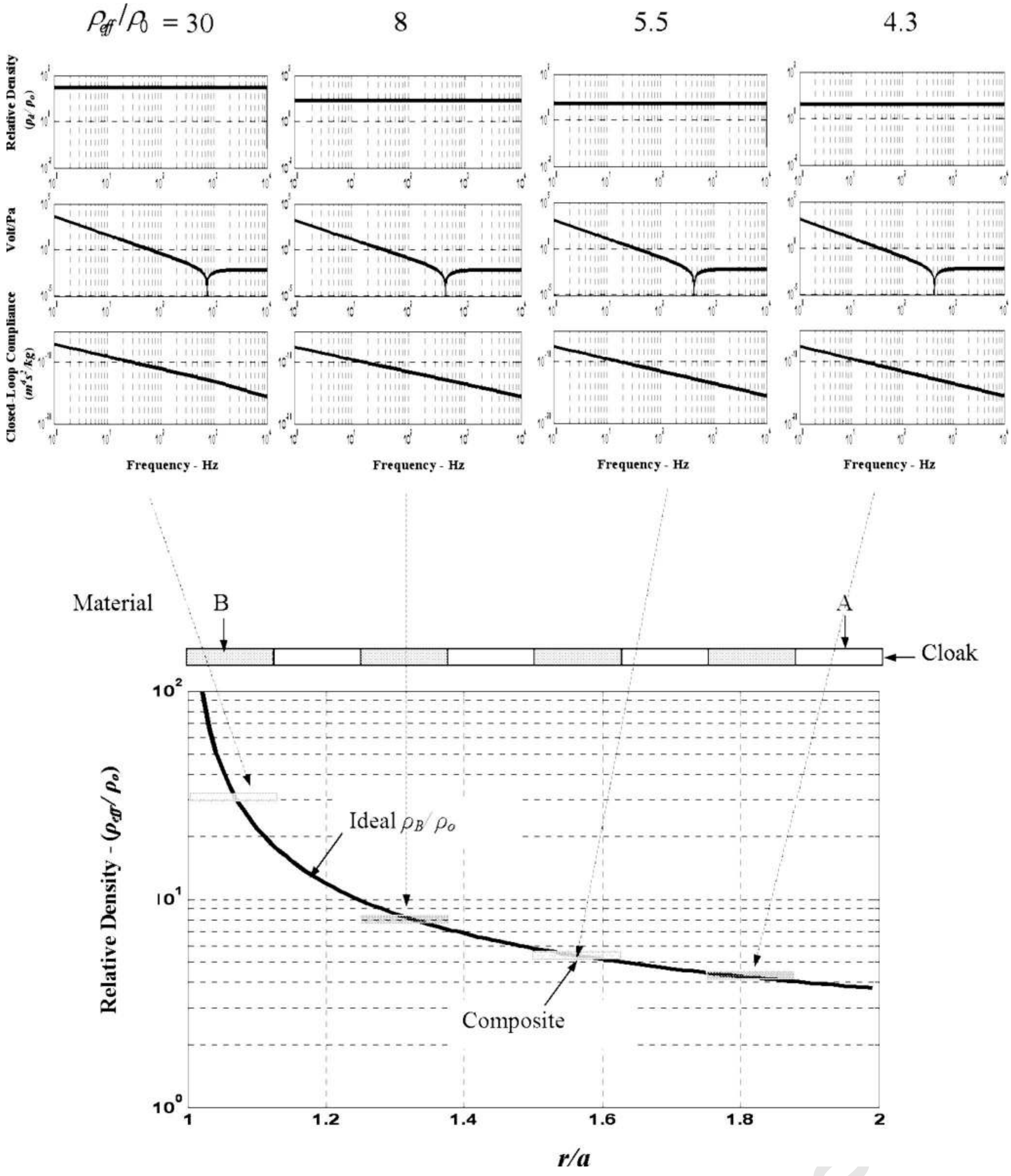

Fig. 11 Active acoustic metamaterial (B) with decreasing density distribution

E = electrical field
G = feedback gain
k_D = diaphragm stiffness
L_C = inductance of cavity
l = length of cavity
M_D = mass of diaphragm
p = fluid pressure in the time domain
P = fluid pressure in the Laplace domain
Δp = pressure drop along cavity
Δp_P = pressure across piezoelectric diaphragm
Q = volumetric flow rate
q = electrical charge
R = radius of diaphragm
S = strain
s^E = piezoelectric compliance
s = Laplace complex number

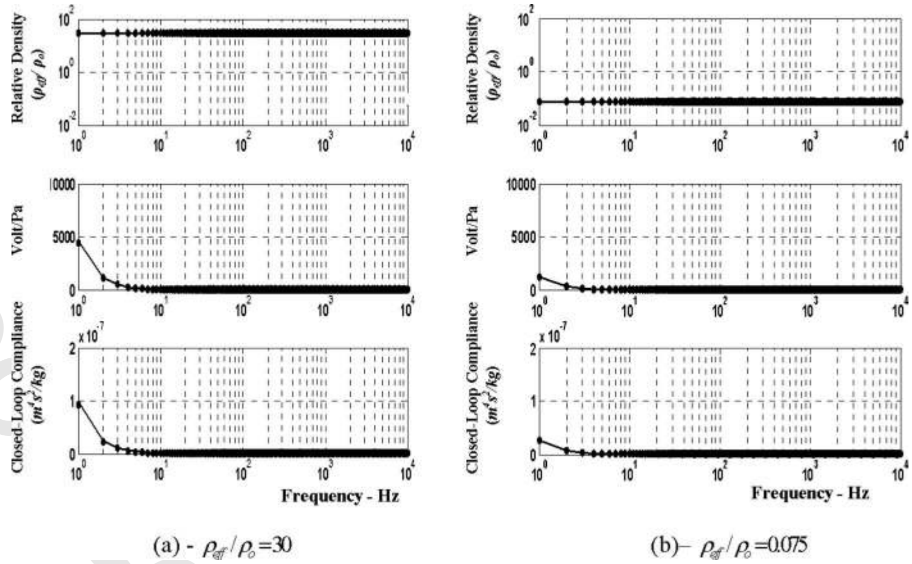

Fig. 12 Comparisons between the predictions of the full (exact) and reduced-order (approximate) feedback gain models (— exact, ● approximate)

T = stress
t = diaphragm thickness
u = flow velocity
V = volume of cavity
V_P = piezoelectric voltage
ΔVol = volume change of diaphragm
Z_P = Impedance of piezoelectric diaphragm and attachments

Greek Symbols

ε = permittivity
κ = bulk modulus of fluid
κ' = dimensionless bulk modulus (κ/κ_o)
λ = wavelength
ρ = density of fluid
ρ' = dimensionless density (ρ/ρ_o)
ϕ = electrical to acoustic domain transformer turn ratio
ω = frequency

Subscripts

d = desired
o = ambient fluid
eff = effective
P = piezoelectric

References

[1] Lapine, M., 2007, "The Age of Metamaterials," Metamaterials, **1**, p. 1.
[2] Shamonina, E., and Solymar, L., 2007, "Metamaterials: How the Subject Started," Metamaterials, **1**, p. 12–18.
[3] Gil, M., Bonache, J., and Martín, F., 2008, "Metamaterial Filters: A Review," Metamaterials, **2**, pp. 186–197.
[4] Milton, G. W., Briane, M., and Willis, J. R., 2006, "On Cloaking for Elasticity and Physical Equations With a Transformation Invariant Form," New J. Phys., **8**, p. 248.
[5] Cummer, S. A., and Schurig, D., 2007, "One Path to Acoustic Cloaking," New J. Phys., **9**, p. 45.
[6] Cummer, S. A., Rahm, M., and Schurig, D., 2008a, "Material Parameters and Vector Scaling in Transformation Acoustics," New J. Phys., **10**, p. 115025.
[7] Norris, A. N., 2008, "Acoustic Cloaking Theory," Proc. R. Soc., Math. Phys. Eng. Sci., **464**(2097), pp. 2411–2434.
[8] Torrent, D., and Sánchez-Dehesa, J., 2007, "Acoustic Metamaterials for New Two Dimensional Sonic Devices," New J. Phys., **9**, p. 323.
[9] Torrent, D., and Sánchez-Dehesa, J., 2008, "Acoustic Cloaking in Two Dimensions: A Feasible Approach," New J. Phys., **10**, p. 063015.
[10] Popa, B. I., and Cummer, S., 2009, "Cloaking With Optimized Homogenous Anistropic Layers," Phys. Rev. A, **79**, p. 023806.
[11] Cheng, Y., Yang, F., Xu, J. Y., and Liu, X. J., 2008, "A Multilayer Structured Acoustic Cloak With Homogeneous Isotropic Materials," Appl. Phys. Lett., **92**, p. 151913.
[12] Cheng, Y., Xu, J. Y., and Liu, X. J., 2008, "One-Dimensional Structured Ultrasonic Metamaterials With Simultaneously Negative Dynamic Density and Modulus," Phys. Rev. B, **77**, p. 045134.
[13] Cheng, Y., and Liu, X. J., 2009, ""Three Dimensional Multilayered Acoustic Cloak With Homogeneous Isotropic Materials," Appl. Phys. A: Mater. Sci. Process., **94**(1), pp. 25–30.
[14] Chen, H.-Y., Yang, T., Luo, X.-D., and Ma, H.-R., 2008, "Impedance-Matched Reduced Acoustic Cloaking With Realizable Mass and Its Layered Design," Chin. Phys. Lett., **25**(10), pp. 3696–3699.
[15] Cummer, S. A., Popa, B.-I., Schurig, D., Smith, D. R., Pendry, J., Rahm, M., and Starr, A., 2008b, "Scattering Derivation of a 3D Acoustic Cloaking Shell," Phys. Rev. Lett., **100**, p. 024301.
[16] Pendry, J. B., and Li, J., 2008, "An Acoustic Metafluid: Realizing a Broadband Acoustic Cloak," New J. Phys., **10**, p. 115032.
[17] Norris, A. N., 2009, "Acoustic Metafluids," J. Acoust. Soc. Am., **125**(2), pp. 839–849.
[18] Lee, S. H., Park, C. M., Seo, Y. M., Wang, Z. G., and Kim, C. K., 2009a, "Negative Effective Density in an Acoustic Metamaterial," arXiv:cond-mat/0812.2954v3.
[19] Lee, S. H., Park, C. M., Seo, Y. M., Wang, Z. G., and Kim, C. K., 2009b, "Reverse Doppler Effect of Sound," arXiv:cond-mat/0901.2772v2.
[20] Yao, S., Zhou, X., and Hu, G., 2008, "Experimental Study on Negative Effective Mass in a 1D Mass–Spring System," New J. Phys., **10**, p. 043020.
[21] Kinsler, L., Frey, A., Coppens, A., and Sanders, J., 2000, *Fundamentals of Acoustics*, 4th ed., Wiley, New York.
[22] Blauert, J., and Xiang, N., 2008, *Acoustics for Engineers*, Springer-Verlag, Berlin.
[23] ANSI/IEEE, 1987, "American National Standards/Institute of Electrical and Electronics Engineers "Standard on Piezoelectricity"," *ANSI/IEEE STD:176-1987*, IEEE, New York.
[24] Prasad, S., Gallas, Q., Horowitz, S., Homeijer, B., Sankar, B., Cattafesta, L., and Sheplak, M., 2006, "Analytical Electroacoustic Model of a Piezoelectric Composite Circular Plate," AIAA J., **44**(10), pp. 2311–2318.

PROOF COPY [VIB-09-1159] 017002VAJ